EL2-like defects in InP nanowires: An *ab initio* total energy investigation

R. H. Miwa and T. M. Schmidt
Instituto de Física, Universidade Federal de Uberlândia, Caixa Postale 593, 38400-902 Uberlândia, Minas Gerais, Brazil

A. Fazzio
Instituto de Física, Universidade de São Paulo, Caixa Postale 66318, 05315-970 São Paulo, São Paulo, Brazil

(Received 7 December 2006; published 26 April 2007)

We have performed an *ab initio* total energy investigation, within the density-functional theory, of antisite defects in InP nanowires (InP NWs) grown along the [111] direction. Our total energy results indicate that (i) P antisites (P_{In}) are the most likely antisite defect compared with In antisites (In_P) and (ii) the formation energies of P and In antisites do not depend on the NW diameter. In particular, in thin InP NWs, with diameters of ~13 Å, the P_{In} antisite exhibits a trigonal symmetry, lying at 0.15 Å from the T_d site, followed by a metastable configuration with P_{In} in an interstitial position (1.15 Å from the T_d site). We find a P_{In}-P dissociation energy of 0.33 eV, and there is no EL2-like center for such a thin InP NW. However, EL2-like defects occur by increasing the NW diameter. For diameters of ~18 Å, the P_{In}-P dissociation energy increases to 0.53 eV, which is 0.34 eV lower compared with the P_{In}-P dissociation energy for the InP bulk phase, 0.87 eV. We mapped the atomic displacements and calculated the relaxation energy, Franck-Condon shift, upon single excitation of P_{In} induced states in InP NW. The formation (or not) of EL2-like defects, P_{In} dissociation energy barrier, and the Franck-Condon energy shift can be tuned by the NW diameter.

DOI: 10.1103/PhysRevB.75.165324 PACS number(s): 71.15.Mb, 71.15.Nc, 71.20.−b

I. INTRODUCTION

Antisite is one of the most studied native defect in III-V compounds, for instance, the EL2 center in GaAs. In a seminal work, Kamińska *et al.*[1] established that the EL2 center exhibits a tetrahedral symmetry formed by an isolated As antisite defect (As_{Ga}). Afterward, several experimental[2,3] as well as theoretical studies[4–8] have been done aiming to clarify the structural and electronic properties of EL2 in GaAs. After more than ten years of investigations, currently there is a general agreement that the stable EL2 center is ruled by an isolated As_{Ga} with a T_d symmetry, while the metastable configuration ($EL2^M$) is attributed to the As_{Ga} atom displaced along the C_{3v} axis.

It is well known that the low-temperature growth of other III-V semiconductors, not only GaAs, allows the preparation of highly nonstoichiometric compounds. Indeed, anion-antisite defects in InP, P_{In}, has been identified for the first time unambiguously through the electron paramagnetic resonance technique by Kenedy and Wilsey.[9] Dreszer *et al.*,[10] using Hall, high-pressure far-infrared absorption and optically detected magnetic-resonance measurements (at low temperature), verified that InP has two dominant donor levels associated with phosphorus antisite defects. Further investigations, based on *ab initio* total energy calculations, proposed the formation of P_{In} antisite clusters in the InP bulk.[11]

The most interesting property on this class of defects is the fact that they also exhibit a clear metastable behavior.[4,12,13] A neutral anion-antisite defect in III-V compounds has a stable fourfold and a metastable threefold interstitial configuration, where the anion antisite is displaced along the C_{3v} axis,[13] similarly to EL2 and $EL2^M$ defects observed in GaAs. This center can be photoexcited into a metastable state, from which it returns to the ground state by thermal activation. Thus, a persistent photoconductivity is expected for P_{In} at low temperature.

Nowadays the electronic properties of several materials can be tailored throughout the manipulation and/or control of their size in the atomic scale. Within this new class of (nano)structured materials, the semiconductor nanowires (NWs) are attracting a great deal of interest for future applications in several types of nanodevices. In particular, InP nanowires (InP NWs) have been considered as a potential structure for the fabrication of sensors, light-emitting diodes, and field-effect transistors.[14,15] Usually, the vapor-liquid-solid mechanism, with a gold particle seed, has been utilized for the growth of these nanostructures.[16] These materials are quasi-one-dimensional with electrons confined perpendicularly to the NW growth direction. They exhibit interesting electronic and optical properties due to quantum confinement effects, viz., the size dependence of the InP NW band gap.[17,18] Recent *ab initio* calculations, performed by Li *et al.*,[19] suggested the formation of a stable *DX* center in small GaAs quantum dots, with dot diameter smaller than ~15 nm.

It is quite likely that native defects would form during the NW growth process. Therefore, the structural and electronic properties of these defects are important issues to be addressed in order to improve our understanding of native defects in quasi-one-dimensional (quasi-1D) semiconducting NW systems.

In this paper, we carried out an *ab initio* total energy investigation of antisite defects in InP NWs. We find that the formation of EL2-like defects, antisite dissociation energy, and the Franck-Condon (FC) energy are ruled by the NW diameter. On the other hand, the antisite formation energies are insensitive to the NW diameter, P_{In} antisites being the most likely defect compared with In_P. At the equilibrium geometry, the P_{In} atom in thin InP NW (diameter of 13 Å) exhibits an energetically stable trigonal symmetry, followed by a metastable configuration with P_{In} in an interstitial position, 1.15 Å from the T_d site. In this case, the P_{In}-P dissocia-

tion energy is 0.33 eV. Increasing the NW diameter (13 $\rightarrow$18 Å), we find a P_{In}-P dissociation energy of 0.53 eV, where P_{In} lying on the T_d site represents the energetically most stable configuration. For the InP bulk phase, the P_{In}-P dissociation energy is equal to 0.87 eV. Similar to the bulk phase, P_{In} in InP NW induces the formation of localized states within the energy band gap. However, for such a thin NW system, this defect does not exhibit an EL2-like behavior. On the other hand, by increasing the NW diameter, EL2-like defects are expected to occur. Finally, within a constrained density-functional approach,[20] we map the atomic displacements along the InP NW upon single excitation of P_{In} induced states and calculate the respective relaxation energy, FC shift.

II. THEORETICAL APPROACH

Our calculations were performed in the framework of the density-functional theory (DFT),[21] within the generalized gradient approximation due to Perdew *et al.*.[22] The electron-ion interaction was treated by using norm-conserving, *ab initio*, fully separable pseudopotentials.[23] The Kohn-Sham wave functions were expanded in a combination of pseudo-atomic numerical orbitals.[24] A double zeta basis set including polarization functions was employed to describe the valence electrons.[25] The self-consistent total charge density was obtained by using the SIESTA code.[26] The InP NW was modeled within the supercell approach, where the InP bilayers were piled up along the [111] direction with a periodicity length of $2\sqrt{3}a$ and diameters of 13 and 18 Å (a represents the optimized lattice constant along the [111] direction of InP NW). The NW surface dangling bonds were saturated with hydrogen atoms. A mesh cutoff of 170 Ry was used for the reciprocal-space expansion of the total charge density, and the Brillouin zone was sampled by using one special **k** point. We have verified the convergence of our results with respect to the number and choice of the special **k** points. All atoms of the nanowire were fully relaxed within a force convergence criterion of 20 meV/Å.

III. RESULTS AND COMMENTS

Figure 1 presents the atomic structure of the thinnest InP NW, with a diameter of 13 Å and growth along the [111] direction (see top view [Fig. 1(a)] and side view [Fig. 1(b)]) (the hydrogen atoms are not shown). Due to the 1D quantum confinement, perpendicular to the NW growth direction, the energy gap of the InP NW increases compared with the bulk InP (1.0 eV).[18] We find energy gaps of 2.8 and 2.2 eV for NW diameters of 13 and 18 Å, respectively. It is important to take into account that those energy gaps are underestimated, with respect to the experimental measurements, within the DFT approach. Figure 2(a) presents the electronic band structure of the thinnest InP NW for wave vectors parallel to the [111] direction (ΓL direction). At the Γ point, the highest occupied states exhibit an energy split of 0.31 and 0.20 eV (a_1+e) for NW diameters of 13 and 18 Å, respectively. The valence-band maximum of bulk InP is described by a three-fold degenerated t_2 state. Such ($t_2 \rightarrow a_1+e$) energy splitting is due to the $T_d \rightarrow C_{3v}$ symmetry lowering of InP NW with respect to the bulk phase.

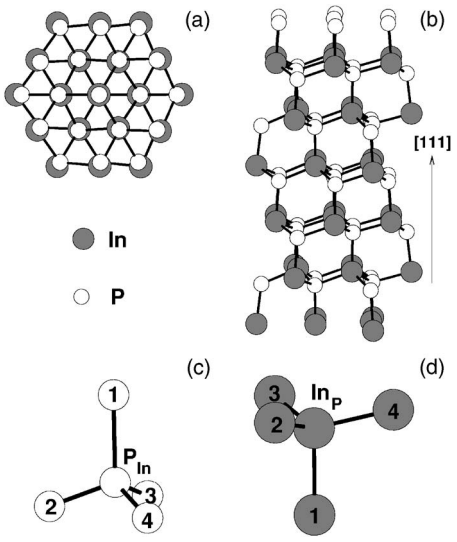

FIG. 1. Structural models of the thinnest InP NW, with a diameter of 13 Å. (a) Top view and (b) side view. The atomic geometry around the antisite defects are indicated in (c) P_{In} and (d) In_P.

The energetic stability of antisites in InP NWs can be examined by the calculation of formation energies. The formation energy (Ω_i) of P and In antisites, Figs. 1(c) and 1(d), respectively, can be written as

$$\Omega_i = E(\mathrm{InPNW}_i) - E(\mathrm{InPNW}) - n_{\mathrm{In}}\mu_{\mathrm{In}} - n_{\mathrm{P}}\mu_{\mathrm{P}}.$$

We have considered the formation of antisite inner InP NWs. $E(\mathrm{InPNW}_i)$ represents the total energy of InP NW, with i=P_{In} or In_P antisite defect, and E(InPNW) is the total energy of a perfect InP NW. n_{In} (n_P) denotes the number of In (P) atoms in excess or in deficiency. The In and P chemical potentials, μ_{In} and μ_P, respectively, are constrained by following the thermodynamic equilibrium condition, $\mu_{In}+\mu_P=\mu_{InP}^{bulk}$, where μ_{InP}^{bulk} is the chemical potential of bulk InP.

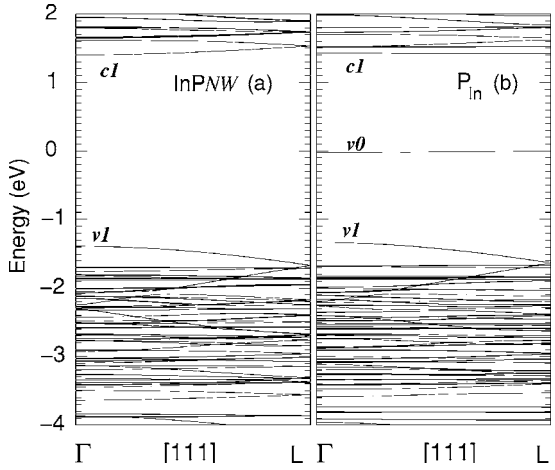

FIG. 2. Electronic band structures of (a) perfect thin InP NW and (b) defective thin InP NW with a P antisite (P_{In}). NW diameter of 13 Å.

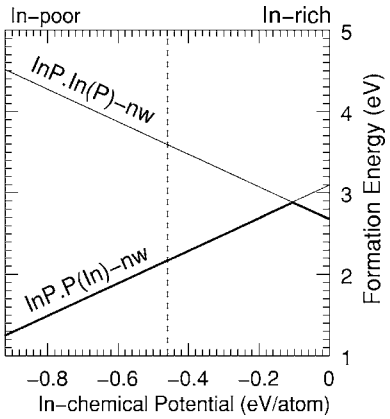

FIG. 3. Formation energies of P_{In} and In_P antisites in thin InP NW, with a diameter of 13 Å, as a function of In chemical potential.

Under an In rich (P poor) condition we will have $\mu_{In} \rightarrow \mu_{In}^{bulk}$, whereas under an In poor (P rich) condition, $\mu_{In} \rightarrow \mu_{In}^{bulk} - \Delta H_f(\mathrm{InP})$.[27] For the heat of formation of bulk InP, $\Delta H_f(\mathrm{InP})$, we have considered its experimental value, 0.92 eV.

Figure 3 presents our calculated results of Ω_i for the thinnest InP NW (diameter of 13 Å), as a function of the In chemical potential. It is clear that the formation of P_{In} is dominant compared with In_P. This latter defect occurs only for In rich condition. At the In and P stoichiometric conditions (dashed line in Fig. 3) we obtained $\Omega_{P_{In}}=2.15$ eV and $\Omega_{In_P}=3.57$ eV. Increasing the NW diameter (18 Å), we find $\Omega_{P_{In}}=2.18$ eV. Within the same calculation procedure, we obtained similar formation energy results for the InP bulk phase, viz., $\Omega_{P_{In}}=2.14$ eV and $\Omega_{In_P}=3.59$ eV. These results indicate that (i) there is an energetic preference for P_{In} antisites, compared with In_P, for both NW and bulk phases of InP and (ii) the formation energy of P_{In} does not depend on the NW diameter.

At the equilibrium geometry, the P_{In} defect in bulk InP keeps the T_d symmetry with P_{In}-P bond lengths of 2.49 Å, while In_P exhibits a weak Jahn-Teller distortion along the [001] direction. These results are in accordance with previous *ab initio* studies of antisites in InP.[11,28,29] On the other hand, the equilibrium geometry of antisites in thin InP NW is quite different. The P_{In}-P_1 bond, parallel to the NW growth direction, is stretched by 27% compared with the other three P_{In}-P_i bonds, $i=2-4$ in Fig. 1(c). Similarly, for the In_P antisite, In_P-In_1 is stretched by 8.6% compared with the other three In_P-In bonds indicated in Fig. 1(d). Figures 4(a) and 4(b) depict the total charge densities along the P_{In}-P_1 and In_P-In_1 bonds, respectively. In particular, due to the large P_{In}-P_1 bond stretching, P_{In} is weakly bonded to P_1, whereas the other P_{In}-P_2, -P_3, and -P_4 bonds [see Fig. 4(a)] exhibit a strong covalent character. Therefore, different from bulk InP, P_{In} antisites in the NW system exhibit a C_{3v} symmetry, with the P_{In} atom displaced from T_d site by 0.15 Å along the [111] axis. Such a P_{In} displacement, along the C_{3v} axis, has not been observed by increasing the NW diameter to 18 Å. In this case, the P_{In} atom occupies a T_d site and the P_{In}-P bond lengths are equal to 2.49 Å.

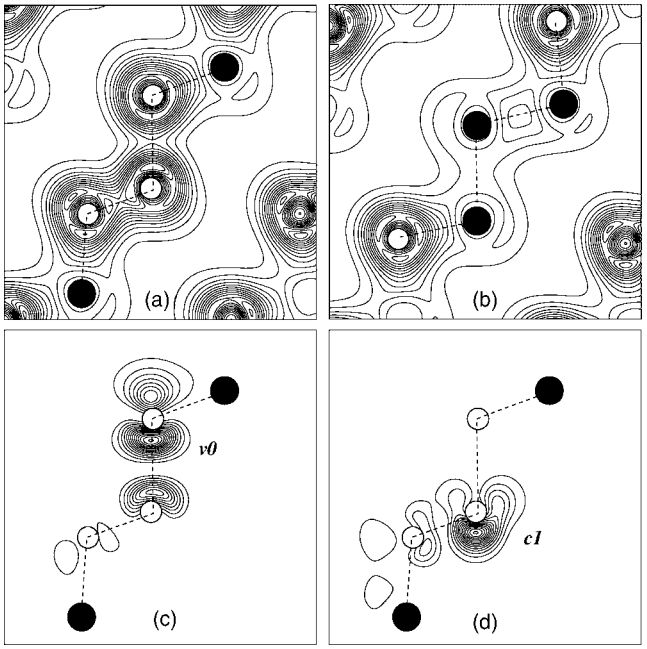

FIG. 4. Total charge densities of (a) P_{In} and (b) In_P antisites in InP NW. The partial charge densities of P_{In} induced (c) highest occupied $v0$ and (d) lowest unoccupied $c1$ states.

Several anion-antisite defects in III-V materials were studied by Caldas *et al.*[13] In that work, based on *ab initio* total energy calculations, the authors observed an energetically stable T_d symmetry for P_{In} and a metastable C_{3v} configuration for the antisite atom displaced by ~1.3 Å along the [111] direction. Indeed, in Fig. 5(a) we present our total energy results as a function of the P_{In} displacement along the [111] direction for the InP bulk phase. We find that the T_d symmetry represents the energetically most stable configuration, followed by an energy barrier of 0.87 eV at 0.7 Å from the T_d site, $z=0.7$ Å, breaking the P_{In}-P_1 bond. Finally, the metastable C_{3v} configuration occurs for $z=1.2$ Å, where the P_{In} occupies an interstitial site. Figures 5(b) and 5(c) present the energy barrier for P_{In} in thin InP NW. We have examined two different processes: (i) The In and P atoms of the NW are not allowed to relax during the P_{In} displacement [Fig. 5(b)]. (ii) The In and P coordinates are fully relaxed for each P_{In} step along the [111] direction, i.e., an adiabatic process [Fig. 5(c)]. It is noticeable that the energy barrier calculated in (i) is very similar to that obtained for P_{In} in bulk InP [Fig. 5(a)]. In (i), the energetically most stable configuration for P_{In} exhibits a T_d symmetry, and we find a dissociation energy of 0.84 eV for $z=0.86$ Å. Further, P_{In} displacement indicates a C_{3v} metastable geometry for $z \approx 1.15$ Å, where the P_{In} atom occupies an interstitial site. Meanwhile, in (ii) the C_{3v} symmetry, with the P_{In} atom lying at 0.15 Å from the T_d site, represents the energetically most stable configuration. The P_{In}-P_1 dissociation energy reduces to 0.33 eV (at $z=0.85$ Å), and there is a metastable geometry for $z \approx 1.15$ Å. The total energy difference between the stable (S) and the metastable (M) configurations, $E(S)-E(M)$, in InP NW is equal to −0.084 eV, while in bulk InP we find $E(S)-E(M)=-0.53$ eV. Comparing (i) and (ii), we verify that the atomic relaxation plays a fundamental role not only for the

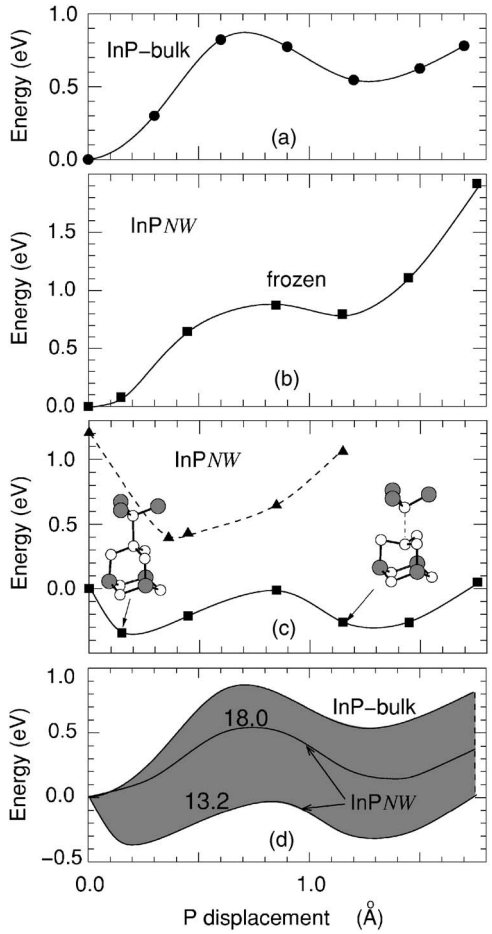

FIG. 5. Total energy as a function of the P_{In} antisite displacement along the [111] direction: (a) bulk InP and (b) InP NW where the In and P atoms are not allowed to relax during the P_{In} displacement. (c) Whole In and P atomic positions along the NW are allowed to relax. In (c), the total energy barrier indicated by triangles (dashed line) was calculated for an excited electronic configuration, single excitation. (d) Energy barriers for bulk InP and thin InP NW systems.

energy barrier for the P_{In} atomic displacement along the [111] direction but also for the equilibrium geometry of the P_{In} structure. Increasing the NW diameter, the energy barrier for the P_{In} displacement will become similar to that obtained for bulk InP (an upper limit for a very large NW diameter) [see Fig. 5(d)]. Indeed, for a NW diameter of 18 Å, we find a P_{In}-P_1 dissociation energy of 0.53 eV and $E(S)-E(M)$ equal to −0.14 eV. These results indicate that the P_{In}-P_1 dissociation barrier, and the $E(S)-E(M)$ total energy difference, can be tuned (by the NW diameter) within the shaded region indicated in Fig. 5(d).

Focusing on the electronic structure, the formation of the P_{In} defect in thin InP NW gives rise to a deep double donor state, labeled $v0$ in Fig. 2(b), lying at 1.3 eV above $v1$. Such a P_{In} induced state is very localized within the fundamental band gap, being almost flat along the ΓL direction. For P_{In} in bulk InP, *ab initio* studies performed by Seitsonen *et al.*[28] indicates the formation of an occupied state at 0.7 eV above the valence-band maximum. The partial charge-density contour plot of $v0$ [Fig. 4(c)] shows an antibonding π^* orbital concentrated along the P_{In}-P_1 bond. The lowest unoccupied state, $c1$, is also concentrated on the P_{In} antisite, as depicted in Fig. 4(d).

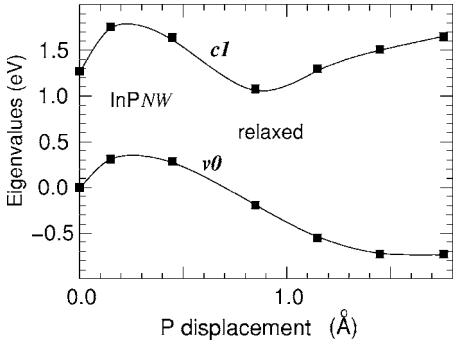

FIG. 6. Single-particle eigenvalues (ϵ) for P_{In}: highest occupied $v0$ [Fig. 4(c)] and lowest unoccupied $c1$ [Fig. 4(d)].

EL2 and $EL2^M$ centers in III-V are characterized by a stable T_d and a metastable C_{3v} geometries for an isolated V_{III} interstitial atom. However, before the V_{III} antisite arrives at the metastable C_{3v} configuration, there is a strong electronic coupling between the highest occupied and the lowest unoccupied antisite induced states near the local maximum for the V_{III}-V dissociation energy (see Fig. 3 in Ref. 13 and Fig. 4 in Ref. 30).

Similarly, for the thin InP NW, we examined the energy positions of single-particle eigenvalues, $\epsilon(v0)$ and $\epsilon(c1)$, as a function of the P_{In} displacement along the C_{3v} axis. Our calculated results, depicted in Fig. 6, reveal that there is no electronic coupling between $v0$ and $c1$. Thus, based on the calculated energy barrier [Fig. 5(c)] and the evolution of the antisite induced states, $v0$ and $c1$, we can state that there is no EL2-like center in thin InP NWs. On the other hand, increasing the NW diameter [Fig. 5(d)], an EL2-like center is expected to occur in InP.

Within the DFT approach, we have examined the structural relaxations upon single excitation from the highest occupied state ($v0$) to the lowest unoccupied state ($c1$) of P_{In} in thin InP NW. We have used the calculation procedure proposed by Artacho *et al.*, where the single excitation was modeled by "promoting an electron from the highest occupied molecular orbital to the lowest unoccupied molecular orbital,"[20] i.e., a "constrained" DFT calculation. Hence, promoting one electron from $v0$ to $c1$, $v0 \rightarrow c1$, we obtained the equilibrium geometry (full relaxations) as well as the self-consistent electronic charge density. The atomic relaxations along the thinnest InP NW, upon $v0 \rightarrow c1$ single excitation, are localized near the P_{In} position. Since we are removing one electron from the antibonding π^* orbital depicted in Fig. 4(c), the P_{In}-P_1 bond shrinks by 0.12 Å (2.90→2.78 Å) and there is a radial a contraction of ~0.2 Å at z=6.8 Å.

The structural relaxations are proportional to the degradation of optical energy due to the atomic displacements associated with such a $v0 \rightarrow c1$ single excitation, FC shift. Comparing the radial and the longitudinal displacements, we verify that most of the FC shifts come from the atomic relaxation parallel to the NW growth direction. The atomic

displacements along the radial direction (Δr) are localized nearby P_{In}, lying within an interval of $-0.2 < \Delta r < 0$ Å, while the atomic displacements parallel to the growth direction (Δz) lie within a range of $-0.2 < \Delta z < 0.3$ Å, being less concentrated around the P_{In} antisite position. We find a FC energy shift of 0.8 eV, which is quite large compared with the InP bulk phase. Within the same calculation approach, we find a FC energy shift of 0.05 eV for InP bulk. Previous *ab initio* study indicates a FC energy shift of 0.1 eV for bulk InP, suggesting thus that the FC energy shift can also be tuned by controlling the NW diameter.

IV. CONCLUSIONS

In summary, we have performed an *ab initio* total energy investigation of antisites in InP NW. We find that the P_{In} antisite is the most likely to occur. For thin InP NWs, the P_{In} atom exhibits a trigonal symmetry, followed by a metastable P interstitial configuration. Increasing the NW diameter (18 Å), P_{In} occupying the T_d site becomes the energetically most stable configuration. The calculated energy barrier, for P_{In} displacement along the C_{3v} axis, indicates that there is no EL2-like defect in thin InP NWs. However, increasing the NW diameter, $13 \rightarrow 18$ Å, we observe the formation of EL2-like defects in InP. Within a constrained DFT approach, we calculated the structural relaxations and the FC energy shift upon single excitation of the electronic states induced by P_{In}. We inferred that not only the formation (or not) of EL2-like defects but also (i) the P_{In}-P dissociation energy, (ii) the total energy difference between stable and metastable P_{In} configurations, $E(S)-E(M)$, and the (iii) FC energy shift can be tuned by controlling the InP NW diameter.

ACKNOWLEDGMENTS

The authors acknowledge the financial support from the Brazilian agencies CNPq, FAPEMIG, and FAPESP. Most of the calculations were performed using the computational facilities of the Centro Nacional de Processamento de Alto Desempenho/CENAPAD-Campinas.

[1] M. Kamińska, M. Skowroński, and W. Kuszko, Phys. Rev. Lett. **55**, 2204 (1985).
[2] H. J. von Bardeleben, D. Stiévenard, D. Deresmes, A. Huber, and J. C. Bourgoin, Phys. Rev. B **34**, 7192 (1986).
[3] D. Kabiraj and S. Ghosh, Appl. Phys. Lett. **87**, 252118 (2005).
[4] D. J. Chadi and K. J. Chang, Phys. Rev. Lett. **60**, 2187 (1988).
[5] J. Dabrowski and M. Scheffler, Phys. Rev. Lett. **60**, 2183 (1988).
[6] Q.-M. Zhang and J. Bernholc, Phys. Rev. B **47**, 1667 (1993).
[7] D. J. Chadi, Phys. Rev. B **68**, 193204 (2003).
[8] H. Overhof and J.-M. Spaeth, Phys. Rev. B **72**, 115205 (2005).
[9] T. Kenedy and N. Wilsey, Appl. Phys. Lett. **44**, 1089 (1984).
[10] P. Dreszer, W. M. Chen, K. Seendripu, J. A. Wolk, W. Walukiewicz, B. W. Liang, C. W. Tu, and E. R. Weber, Phys. Rev. B **47**, 4111 (1993).
[11] T. M. Schmidt, R. H. Miwa, A. Fazzio, and R. Mota, Phys. Rev. B **60**, 16475 (1999).
[12] J. Mikucki, M. Baj, D. Wasik, W. Walukiewicz, W. G. Bi, and C. W. Tu, Phys. Rev. B **61**, 7199 (2000).
[13] M. J. Caldas, J. Dabrowski, A. Fazzio, and M. Scheffler, Phys. Rev. Lett. **65**, 2046 (1990).
[14] J. Wang, M. S. Gudiksen, X. Duan, Y. Cui, and C. M. Lieber, Science **293**, 1455 (2001).
[15] X. Duan, Y. Huang, Y. Cui, J. Wang, and C. M. Lieber, Nature (London) **409**, 66 (2001).
[16] S. Bhunia, T. Kawamura, Y. Watanabe, S. Fujikawa, and K. Tokushima, Appl. Phys. Lett. **83**, 3371 (2003).
[17] H. Yu, J. Li, R. A. Loomis, L.-W. Wang, and W. Buhro, Nat. Mater. **2**, 517 (2003).
[18] T. M. Schmidt, R. H. Miwa, P. Venezuela, and A. Fazzio, Phys. Rev. B **72**, 193404 (2005).
[19] J. Li, S.-H. Wei, and L.-W. Wang, Phys. Rev. Lett. **94**, 185501 (2005).
[20] E. Artacho, M. Rohlfing, M. Côté, P. D. Haynes, R. J. Needs, and C. Molteni, Phys. Rev. Lett. **93**, 116401 (2004).
[21] P. Hohenberg and W. Kohn, Phys. Rev. **136**, B864 (1964).
[22] J. P. Perdew, K. Burke, and M. Ernzerhof, Phys. Rev. Lett. **77**, 3865 (1996).
[23] L. Kleinman and D. M. Bylander, Phys. Rev. Lett. **48**, 1425 (1982).
[24] O. F. Sankey and D. J. Niklewski, Phys. Rev. B **40**, 3979 (1989).
[25] E. Artacho, D. Sánchez-Portal, P. Ordejón, A. Garcia, and J. M. Soler, Phys. Status Solidi B **215**, 809 (1999).
[26] J. M. Soler, E. Artacho, J. D. Gale, A. García, J. Junquera, P. Ordejón, and D. Sánchez-Portal, J. Phys.: Condens. Matter **14**, 2745 (2002).
[27] G.-X. Qian, R. M. Martin, and D. J. Chadi, Phys. Rev. B **38**, 7649 (1988).
[28] A. P. Seitsonen, R. Virkkunen, M. J. Puska, and R. M. Nieminen, Phys. Rev. B **49**, 5253 (1994).
[29] C. W. M. Castleton and S. Mirbt, Phys. Rev. B **70**, 195202 (2004).
[30] J. Dabrowski and M. Scheffler, Phys. Rev. B **40**, 10391 (1989).